Experimental analysis of the flow structure in the laboratory model of SOFC fuel cell channels

M. Jaszczur[1], **G. Pucillo**[1,2], **R. Nowak**[1], **L. Magistri**[2]
[1]AGH University of Science and Technology, Faculty of Energy and Fuels
Department of Fundamental Research in Energy Engineering, Poland
[2]University of Genova, Faculty of Engineering, Italy

E-mail: marek.jaszczur@agh.edu.pl

Abstract. In the presented paper a flow structure in the gas channel of planar SOFC fuel cell is presented. The model taken for analysis was constructed based on the channel geometry manufactured by SOFC Power company. The shape of a channel was rectangular filled with large number of obstacles which role is to divide the flow into segments with possibly homogenous velocity distribution. The model itself was constructed from Plexiglas and the reactant gases flow was modelled by water motion. To investigate and visualize the flow structures a PIV technique was applied. Three different flow rates were taken for investigations and the flow uniformity and time dependence was studied.

1. Introduction

Fuel cells are devices that generate electricity by a chemical reaction. In general, hydrogen is normally used as the basic fuel, which reacts electrochemically with oxygen producing electricity, heat and, as a by product, water. Fuel cells are usually classified by the electrolyte employed in the cell and the main five types are: Alkaline Fuel Cell, Molten Carbonate Fuel Cell, Phosphoric Acid Fuel Cell, Polymer Electrolyte Fuel Cell and Solid Oxide Fuel Cell (SOFC).
A second grouping can be done by looking at the operating temperature for each of the fuel cells. The high-temperature fuel cells operate at temperatures approx. 600±1000°C and two different types have

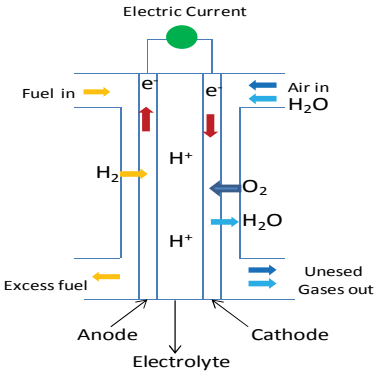

Figure 1. Transport processes within a SOFC

been developed, the Molten Carbonate Fuel Cell and the Solid Oxide Fuel Cell. In this paper, an experimental model of gas distributing channels for planar Solid Oxide Fuel Cell has been tested.
In a planar SOFC, cell components are configured as flat plates which are connected in electrical series. Cell itself consists of electrodes, anode (negative) and cathode (positive), where the reactions which produce the electricity takes place. Between them, there is an electrolyte, which allows the transport of electrically charged particles from one electrode to the other, and a catalyst, which enables and speeds up the reaction.
Technical details of the Solid Oxide fuel cell are given below:

- Operating temperature: 800±1000 °C
- Anode reaction: $H_2+O^2 \rightarrow H_2O+2e^-$
- Cathode reaction: $½\ O_2+2e^- \rightarrow O^2$
- Applications: combined heat and power for stationary decentralised systems and for transportation (trains, boats, etc.)
- Realised Power: small power plants 100-250 kW
- Charge Carrier in the Electrolyte: O^{2-}

In general SOFC cells employ a solid oxide material as electrolyte and are, thus, more stable than the molten carbonate fuel cells as no leakage problems due to a liquid electrolyte can occur. The SOFC cell is a straightforward two-phase gas-solid system so it has no problems with water management, flooding of the catalyst layer, or slow oxygen reduction kinetics. On the other hand it is difficult to find suitable materials which have the necessary thermal and stability properties for operating at high temperatures. An important advantage of SOFCs is the internal reforming. Due to the high temperature of the exhaust gases a combination with other power generation systems (e.g., gas turbines) is also possible which can provide a high overall electrical efficiency (up to 70% in a combined cycle system).

A cell configuration must be designed to have the desired electrical and electrochemical performance, along with required thermal management and mechanical/structural integrity to meet operating requirements of specified power generation applications. The requirements of electrical performance means that the design must minimise ohmic losses in the stack. Thus, the current path in the components must be designed to be as short as possible. Electrochemical performance means that the design must provide the full open circuit voltages and minimal polarisation losses. The gases must be able to quickly reach in the reaction sites to reduce mass transport limitation. The requirement of thermal management means that the cell must provide means for more uniform temperature distribution during operation. Finally, the mechanical/structural integrity means that any planar SOFC stack must be designed to have adequate mechanical strength for assembly and handling.
Different designs for solid oxide fuel cells have been developed over the years. Flat plates have an easier stack configuration while tubular designs have a smaller sealing problem. Due to the high power density of SOFCs compact designs are feasible. The tubular design has been developed by Westinghouse. Tubular designs have a self sealing structure which improves thermal stability and eliminates the need for good thermal-resistant sealants.

The planar design is more efficient and cheaper than the tubular as the current path is shorter and it is easier to stack than the tubular design.
In a SOFC cell there are different plate structures that produce different flow field as, for example, squared spot, serpentine spirals, cascade (this structure uses sealed-off channel that make blockages by water droplets above all it induces a large pressure difference in the cell) and series-parallel, with geometries of various complexity levels. Depending on the concentration of the reactant different flow designs may be advantageous.

The square spot structure in not optimal for an equal distribution of the gases as the reactant gas can flow through the cell by any path available. The advantage of this flow is the fact that the pressure drop is minimal.

In the serpentine configuration (difficult to fabricate if the machining is done manually) reactant gases are obliged to follow the path; therefore a large pressure drops over the gas path may occur and the flow is also affected by impingement, recirculation and flow separation. For this reason it is important to determine the critical Reynolds number necessary for the onset of instability.

J. Martin *et al.* [1] investigated the fluid dynamic phenomena for a model of a U-shaped fuel cell channel and they compared two perpendicular flow planes in terms of absolute and averaged velocity values as well as Reynolds stress correlations. Generally, the flow undergoes a transition to a different regime when two recirculation zones, which originally develop in the U-bend region, merge into one separation region. This transition corresponds to generation of additional vortices in the secondary flow plane. The analytic foundations for secondary flows in curved pipes were given by Dean [2] who established that the onset of secondary vortices in curved pipes is characterized by ratio of Reynolds number to the square of the product of the inertia and centrifugal forces. Hawthorne [3] showed that the secondary flow could occur in a perfectly inviscid flow as a result of a non uniform distribution of velocity at the entrance.

The studies of Martin reveal that at Re<381 the flow in the bend was time independent in both the stream wise and cross-flow planes and was downstream from the bend. At Re>436 the flow in the bend was clearly time dependent in both the stream wise and cross-flow planes and was unstable downstream from the bend. The secondary flow at the midpoint of the turn appeared to contain four major vortices. Besides the ratio of secondary to primary motion was found to decrease after the transition occurred. This suggests that enhanced mixing in the cathode flow channel of fuel cell could be achieved by designing a serpentine channel such that transition occurs around the Reynolds number corresponding on design point operation.

The studies of flow behaviour [4],[5] in cell flow channels were also made in commercial parallel bipolar plate and also in this case the results reveal a non-homogeneous flow distribution across the bipolar plate produce a limited performance of the fuel cell energy conversation.

It is particularly important for the cells with direct internal reforming where the cooperating endothermic reforming reaction, exothermic water gas shift and hydrogen conversation reactions are among those responsible for the rise in the temperature difference along the reaction channels. This phenomenon was studied by Ho *et al.* [6], who observed that fuel cooled by the reforming reaction at the inlet to the cell in gradually warmed up as a consequence of the two above reactions. Moreover, Laurencin *et al.* [7] concluded that the "Nusselt number depends strongly in the geometry of the gas channels"; so the channel design is also responsible for the relationship between the conductive and convective heat transfer in the cell. It is in these grounds that R. Nowak and J. Szmyd [8] tested three kinds of radial flow interconnect configurations for a SOFC, to uncover the possibilities for maintaining the uniform velocity distribution in the channel which directly translates into temperature difference and thermal stresses which can occurs in SOFC cell. They concluded that the most promising geometry for the fuel channel keeps almost constant width along its entire length. In this configuration the velocity field was the most uniform and the smallest velocity gradient along its length were observed.

2. Experimental setup

The main components of the experimental setup are shown in Fig. 2. The flow system consisted of a reservoir with a pump and a flow channel. The PIV system was deployed to acquire data.

During the measurement process the channel was laid on a flat surface with distilled water supplied from the tip of the plate. To excite the tracer particles, which have been added to the fluid, a double cavity Nd: Yag laser has been used and was positioned at a distance of about 90 cm from the axis of the cell model. The cell model has been illuminated through lateral surface of one side and then of the other side. The images of particles motion have been recorded through upper surface of the model, by the CCD camera, with a 50 mm f#8 Nikon lens, placed perpendicularly to the light sheet. This arrangement does not introduce any perspective distortion in the images and eliminates any possible direct reflection of the laser on the CCD camera. Data sets have been recorded for a field of

view of 300 mm x 190 mm. The flow rate of water was controlled by the flow controller, and the particles for PIV were added and mixed with the water in the reservoir.

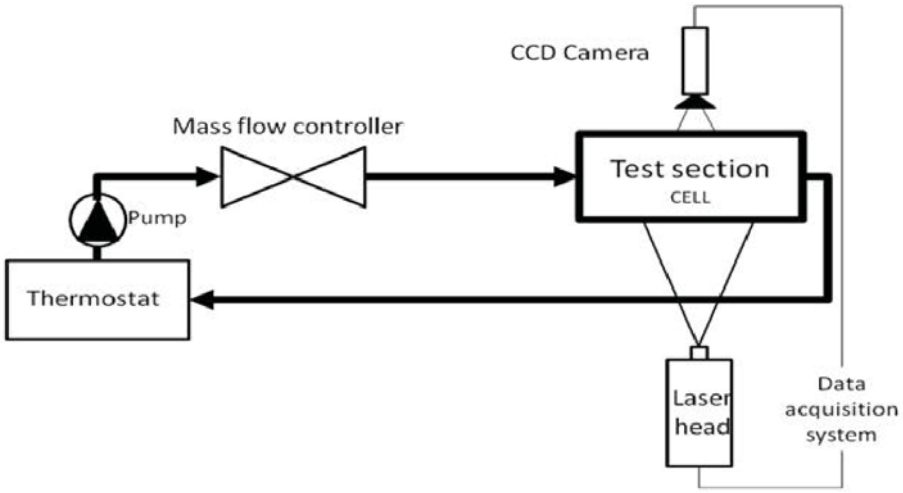

Figure 2. Schematic of the experimental setup

In this paper a rescaled model based on the geometry of the realistic SOFC fuel cell has been tested with four different flow rates. The exact shape of a channel is presented in Figure 3a. The rough surface area, filled with 32 rectangular cross section (1cm x 3 cm) obstacles, was of 378 cm^2 and the thickness of the cell was of 2 cm. The inner diameter of the water supporting tube was approximately 10 mm. Due to the transparency requirements of PIV measurements, the channel was made from a Plexiglas material to allow the investigated flow area to be visible. Because the melting temperature of Plexiglas is about 170°C, it was impossible to carry out the experiment at the high temperatures that characterize SOFC operation. The measurement process was carried out in room temperature and the water motion mixed tracer particles was used as an experimental fluid.

(a)

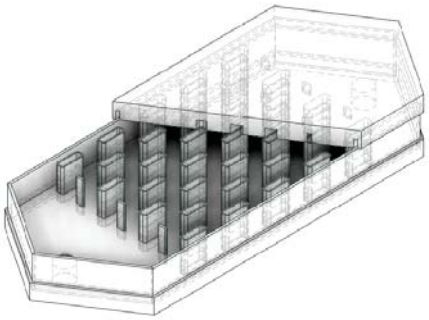

(b)

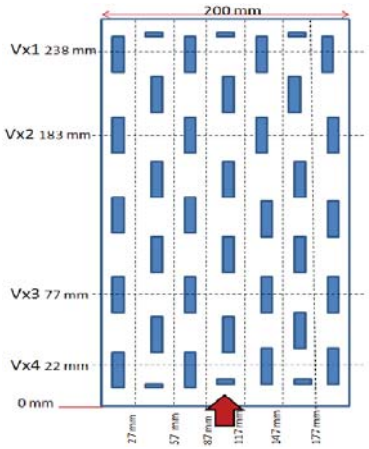

Figure 3. (a) Plexiglass model of SOFC channel, (b) Location of the analysed sections

3. Measurement setup

It was chosen to investigate the flow field inside the channel with the optical measurement technique called Particle Image Velocimetry (PIV). PIV is one of the most recent techniques which allow to determine the instantaneous velocity fields by measuring the displacements of numerous fine particles that accurately follow the motion of the fluid. The PIV method is getting more and more popular in experimental investigations due to its two main advantages: it not interfere with the flow and as a result returns a global measure of the flow field, unlike all the other measurement techniques (except Global Doppler Velocimetry) that allow to perform point measurements.

The standard planar PIV system consists of a double-pulsed laser, light-sheet-forming optics, particle seeding, a monoscopic (single-lens) camera, image digitization hardware and a computer for data storage and analysis.

Double-pulsed illumination is the current norm in PIV because of the ability in using more than two laser pulses. The intensity of illumination required to form visible images of micrometer-sized particles usually requires the use of pulsed solid-state laser sources emitting pulses with energy between 5 and 500 mJ. The energy needed is closely coupled with the scattering properties of the particles.

The flow should be seeded with particles that are small enough to follow the fluid acceleration but large enough to scatter light energy sufficient to form bright images, usually a few tens micrometers in a liquid. The best PIV results are obtained by using artificially seeded particles, thereby permitting careful control of the uniformity of the particle concentration and the optical and fluid mechanical properties of the particles. Particles offer important advantages as markers of the fluid. They produce a stronger optical image than dyed fluid; they are small, of order 0.1-50 μm; they do not diffuse and a solid particles do not deform. It is best to use spherical particles because their images are independent of particle rotation, and barring camera aberrations, the centred of the particle image corresponds to the centre of mass of the particle. The disadvantage of particle markers is that they must slip with respect to the fluid in order to generate the drag force needed to follow the fluid acceleration.

In PIV it is important to strive to achieve a uniform dispersion of scattering particles throughout all regions of the flow that pass though the measurement domain, so as to avoid preferentially sampling selected regions of the velocity field and thereby biasing measurements toward more highly seeded regions.

In PIV the tracer particles are illuminated, by the sheet of laser light, in a plane of measurement in two successive moments of time. The reflected light from the particles is recorded by the sensor of a digital camera , getting two separate frames which will be further processed; the laser must therefore be sufficiently powerful to be able to " impress " the sensor of the digital camera with the small light scattered by small tracer particles , but also must be able to produce a light pulse of short duration, in order to " freeze" the motion of the particles during the exposure and to prevent playback of the image trails . The delay time between two light pulses is a function of the flow velocity: it must be sufficient to identify the displacement of the particles between the two digital images which will act on the software. If the interval is too short, the shift is too small and the noise, due to the "noise" and to the imperfect correlation between the pairs of images, become preponderant compared to the actual displacement.

4. Experimental Results

The measurements of flow velocity distribution in the presented geometry have been performed for four different flow rates ($2{,}44\cdot10^{-5}m^3/s$; $2{,}32\cdot10^{-5}m^3/s$; $3=8{,}91\cdot10^{-6}m^3/s$; $4{,}98\cdot10^{-6}m^3/s$) which correspond to Reynolds numbers (calculated in the section of the inlet tube) of Re=3101, 2948, 1132 and 632. All the statistical calculations were carried out using DaVis 7.2 software. For each flow rate a set of 300 images was recorded. In Figure 4 an average velocity distribution for a case of $2{,}32\cdot10^{-5}m^3/s$

and $4{,}98 \cdot 10^{-6} m^3/s$, corresponding to Reynolds numbers of 2948 and 632 is presented. The average field distribution for the other cases are quite similar to the presented ones.

While analysing the obtained results, it is immediately evident that using lower flow rates, the fluid is less affected by the negative influence of obstacles. The regions with much lower velocities occur mostly in the layers close to the side walls. The side walls caused the flow velocity to decrease mostly in the low flow rate where the general velocity gradient is small.

For the Flow 4 case a good velocity distribution almost all over the channel is obtained with the exception of the lower part near the entrance of the jet. Near the bottom of the channel, a low velocity zone is observed in the flow field, mostly close to the middle and right section of the channel. This low-velocity zone is present in all different flow rates but, as can be verified from the average field distribution, in the higher Reynolds number, is more pronounced. Also the distribution of the flow (for all flow rates) in this part of the channel is evidently not homogenous. It's interesting to note that although the cell structure is assumed to be symmetrical, the measurements results are not completely symmetrical. It has been verified that for all investigated cases, the flow moves with the higher velocities through the left lateral channels. In this part of the channel the velocities are in the range of 0,020-0,023 m/s for higher flow rate and 0,0035-0,0045 for the lower one.

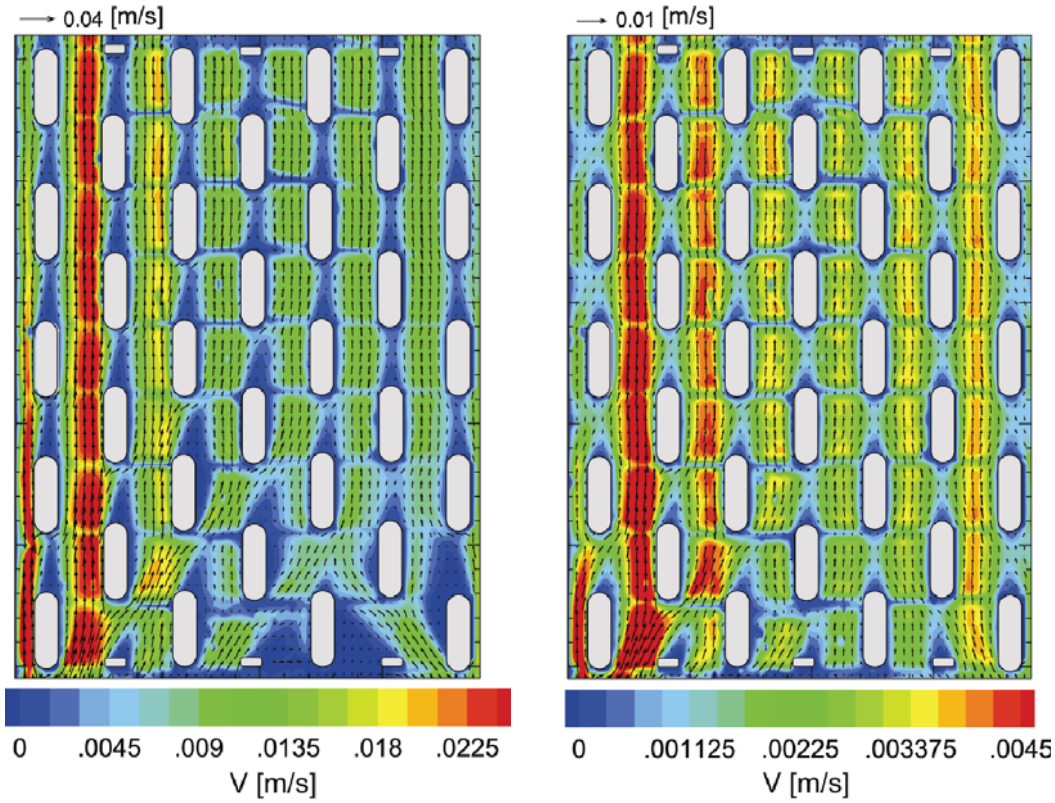

Figure 4. Velocity distribution in the investigated channel; (left) Re=2948, (right) Re=632.

Moreover, the visualized flow is characterized by large velocity gradients in the left part of the channel. It was pointed out that the decrease in velocity is higher for higher flow rates with a gradient of about 0,018 m/s and a gradient of 0,0034 m/s for the lowest flow rate. The higher velocity reached with the case Re=632 about the lower reached with the case Re=2948. On the other hand, inside the channel, the flow is better controlled and is more homogenous with the lower flow rate.

To carry out a more detailed flow structure analysis, the test section was divided transversally by four horizontal sections where the velocity field profiles were calculated. The graphs in Figure 6 show the trend of the velocity, corresponding to the different flow rates, in various stretch of each horizontal section of the channel; obviously the velocity in all sections increased along with the flow rate.

In this case again, the sections most problematic are those nearest the entrance of the jet and in particular in the stretch of width's cell between 70 mm and 120 mm (see in Figure 5b). Curious is the considerable lowering of the velocity to approximately half of each stroke considered; probably the flow is affected by the presence of the obstacle placed in the section above that which is considered. As it has been discussed previously, even the plots indicate the maximum of the fluid velocity is located in the left side of the channel for all different flow rates.

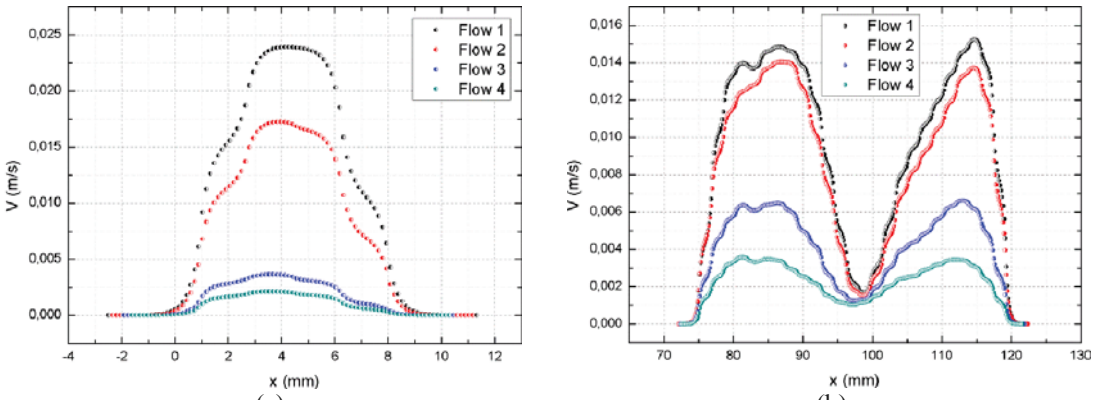

(a) (b)

Figure 5. Comparison of velocity profiles between various Flow rates – Section Vx2.

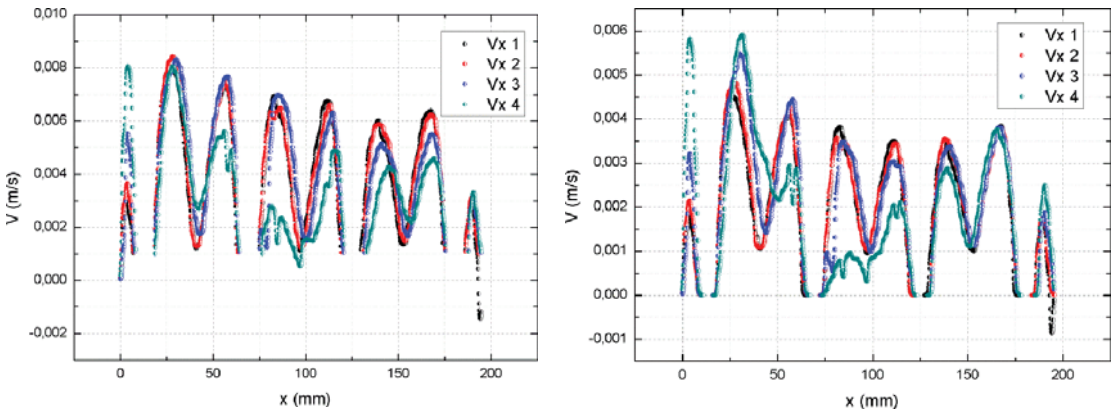

(a) (b)

Figure 6. Comparison of velocity profiles between various sections along the channel; (a) Re=1132, (b) Re=632

The graphs in Figure 6 show, at constant flow rate, the trend of the velocity in four different horizontal sections of the cell (the location of each section is presented in figure 3b). The velocities development for the three sections positioned far from the inlet is very similar, this means that there are not high losses during the crossing of the cell. More problematic and with an anomalous trend (especially at half the width of the channel, where the entrance of the jest is positioned) is instead the trend of the velocity in the lowest section, where probably the flow is heavily influenced by the

presence of three small obstacles erected between the four standard dimensions obstacles. This is especially visible in the highest flow rates where the amplitude of the oscillations increases. Moreover, the velocity difference between the inlet and the outlet of the channel grows for higher flow rates.

As it has been showed in Figure 6, the existence of flow back in the section at the entrance of the channel can also be observed. This phenomena gradually disappears in the above sections and it is less pronounced in the low rates. The reason is probably the influence of the proximity of the inlet of the fluid and the presence of the three small obstacles placed in the bottom section. Very suspicious is a remarkable reversal of the velocity (present in all flow rates) at the highest section, near the right side wall of the channel. Additional measurements have to be performed to verify this phenomenon.

5. Conclusions

In the presented paper an experimental investigation of the flow in the model of SOFC cell gas channel have been performed. A velocity vector fields for two selected flow rates and the velocity plots in various locations of the channel have been shown. The results showed that the flow in such geometry was better controlled for lower flow rates. It was also found that the velocity distribution itself was not fully homogenous. Especially, significantly larger velocities were observed in the regions next to the channel left wall. Additionally an undesirable disturbances of the flow field were caused by the small obstacles located just in the inlet to the channel. However to get a better understanding of the obtained results, additional analysis should be performed in the future works.

Acknowledgements
The present work was supported by the Polish Ministry of Science (Grant AGH No. 11.11.210.198)

References

[1] Martin J., Oshkai P., Djilali N., 2005, “Flow Structures in a U-Shaped Fuel cell Flow Channel: Quantitative Visualization Using Particle Image Velocimetry”, Journal of Fuel Cell Science and Technology, 2, 70-80
[2] Dean, W.R., 1928, “Fluid Motion in a Curved Channel”, Proc. R. Soc. London, Ser. A, 121, 402-420
[3] Hawthorne, W.R., 1951, “Secondary Circulation in Fluid Flow”, Proc. R. Soc. London, Ser. A, 206, 374-387
[4] Nishino T., Szmyd J., 2010, “Numerical analysis of a cell-based indirect internal reforming tubular SOFC operating with biogas”, Journal of Fuel Cell Science and Technology, 7 , 051004-1–051004-8
[5] Nowak R., Szmyd J, 2010, “An experimental analysis of transport phenomena in a models of circular-planar SOFC”, 19th Polish National Fluid Dynamics Conference, 5-9. September, Poznań, Poland
[6] Ho T.X. Kosinski P., Hoffmann A.C., Vik A., 2008, “Numerical study of an SOFC with direct internal reforming using charge diffusion-based model”, Proceeding of 8th European SOFC Forum Lucerne, 1-13
[7] Laucerin J., Morel B., Bulter Y., Lefebvre-Joud F., 2006, “Thermomechanical model of solid oxide fuel cell fed with methane”, Fuel Cells, 6, 64-70
[8] Nowak R., Szmyd J.S., 2011, “An experimental analysis of the flow structure in varius configurations of a circular-planar SOFC fuel channel”, Journal of theoretical and applied mechanics, 49, 541-564